Original Study

Open Access

Brahim Lafifi*, Ammar Rouaiguia, El Alia Soltani

A Novel Method for Optimizing Parameters influencing the Bearing Capacity of Geosynthetic Reinforced Sand Using RSM, ANN, and Multi-objective Genetic Algorithm

https://doi.org/10.2478/sgem-2023-0006
received May 21, 2022; accepted April 3, 2023.

Abstract: In this study, a novel method is proposed to optimize the reinforced parameters influencing the bearing capacity of a shallow square foundation resting on sandy soil reinforced with geosynthetic. The parameters to be optimized are reinforcement length (L), the number of reinforcement layers (*N*), the depth of the topmost layer of geosynthetic (U), and the vertical distance between two reinforcement layers (X). To achieve this objective, 25 laboratory small-scale model tests were conducted on reinforced sand. This laboratory-scale model has used two geosynthetics as reinforcement materials and one sandy soil. Firstly, the effect of reinforcement parameters on the bearing load was investigated using the analysis of variance (ANOVA). Both response surface methodology (RSM) and artificial neural networks (ANN) tools were applied and compared to model bearing capacity. Finally, the multiobjective genetic algorithm (MOGA) coupled with RSM and ANN models was used to solve multi objective optimization problems. The design of bearing capacity is considered a multi-objective optimization problem. In this regard, the two conflicting objectives are the need to maximize bearing capacity and minimize the cost. According to the obtained results, an informed decision regarding the design of the bearing capacity of reinforced sand is reached.

Keywords: Bearing capacity; model tests; square footing; geosynthetic; RSM; ANN; multi objective optimization.

***Corresponding author: Brahim Lafifi,** Laboratory of Civil Engineering and Hydraulics, University 8 Mai 1945 Guelma, Guelma, Algeria, E-mail: blafifi@gmx.fr
Ammar Rouaiguia, El Alia Soltani, Laboratory of Civil Engineering and Hydraulics, University 8 Mai 1945 Guelma, Guelma, Algeria

1 Introduction

The major problem encountered in building shallow foundations resting on loose sand deposits is often the low bearing capacity and excessive settlement. This issue could directly affect the durability and performance of the superstructure. As a possible solution to this problem, replace loose soil with suitable backfill material, increase the area of the footings, or use both keys simultaneously. Indeed, these techniques improve the mechanical properties of the foundation system but with significant construction costs. So, new methods with a suitable solution can be proposed. To ensure good technical qualities at an economical price, it will be using soil reinforcement with geosynthetics [1].

The benefit of using geosynthetic reinforcement in geotechnical engineering projects is to improve the quality of the subgrade of shallow foundations and contribute to an increase in bearing capacity and limitation of settlement. This technique has emerged not today, but over the last three decades. During this period, several works have been carried out either in the laboratory on physical models or as *in situ* tests to study these new reinforcement materials [2].

The first study on the influence of a strip metallic reinforcement to improve the bearing load of a strip foundation was conducted by Binquet and Lee [3, 4]. Then, many investigations have been conducted using a laboratory-scale model for the object to improve the load capacity of shallow foundations resting on reinforced sand. Several materials were used as reinforcement, such as geotextile layers [5–7], geogrids[8–14], strips of metal[15, 16], fibers[17, 18], geocell [19, 20], and geosynthetic reinforcement having wraparound ends [21, 22].

The main objective of the previous works is to study the influence of some parameters related to the bearing capacity of reinforced footing, such as the length of the reinforcements, their number, the depth of the first

layer, and the vertical spacing between layers. The determination of the optimum values of these parameters was also investigated through parametric studies. For example, Fragaszy and Lawton [23] studied the influence of the reinforcement length on the bearing capacity of shallow footing resting on reinforced sand using scale model tests. The obtained results from this work clearly show that an improvement of the load capacity of footing with length varies between 3B and 7B, with B representing the footing width. Concerning the embedment of the first reinforcement layer, Yetimoglu *et al.* [24] conducted studies on footing resting on sandy soil and used only one geogrid layer as reinforcement; they observed that the improvement in bearing capacity occured at an optimum depth of 0.3B.The number of layers was studied by Akinmusuru and Akinbolade [25] using geotextile reinforcement to increase the load capacity of a shallow square foundation. They confirmed that the use of layers reinforcement greater than three had no significant influence on the bearing capacity. So they concluded that the suitable number of reinforcement layers was three with an embedment of the first layer which did not exceed the value of 0.5B (where B is the footing width).

It should be noted that several studies mentioned above regarding the optimization of parameters of reinforcement for bearing capacity have focused only on the parametric studies rather than mathematical models with the use of sophisticated optimization techniques. Therefore, advanced predictive methods seem very helpful in dealing with this problem. Therefore, the use of predicted techniques, such as the response surface method (RSM) [26], artificial neural networks (ANN) [27], genetic algorithms (GA) [28, 29], and neuron fuzzy logic [30], is recommended for the development of a relationship between bearing capacity and designed parameters.

RSM has been used with great success in many fields of civil engineering. It was used to simulate material behavior, optimize of structural problems, for experimental estimation, and to estimate concrete mix proportions. Lafifi *et al.* [31] used the RSM coupled with the Taguchi orthogonal array to optimize the geotechnical parameters of the Mohr–Coulomb model using pressuremeter numerical results. Chana Phutthananon *et al.* [32] also used the RSM coupled with GA as a multiobjective optimization tool to optimize the shape of deep T-shaped mixing and cement deep mixing. The modeling of the micaceous soil was achieved by Zhan *et al.* [33] by using RSM based on linking the unconfined compressive strength with some additives. Recently, Benayoun *et al.* [34] used this tool to investigate the influence of geometric parameters of a nailed wall and identify the influenced parameters on their stability.

Also, the ANN method has shown great success in geotechnical engineering problems. It was in the early 90s that Sasmal and Behera [27] made the first application of ANNs. Kuo *et al.*[35] used this tool to predict the value of the bearing capacity of a strip foundation resting on multi-layered cohesive soil using multi-regression models. Jahed Armaghani *et al.*[36] studied the ANN coupled with the *particle swarm optimization* (PSO) algorithm for modeling the bearing load of socketed piles using 132 data sets. Behera*et al.* [37] predicted the value of the bearing capacity of the strip foundation resting on a horizontal surface and subjected to an eccentric load. Sahu*et al.*[38] estimated the bearing capacity of strip foundations resting on reinforced soil and subjected to an inclined load by the developed ANN model equation. Acharyya and Dey [39] and Acharyya*et al.* [40] presented the prediction of the bearing capacity of a strip foundation located in front of a slope using ANN. Sethy*et al.*[41] predicted the bearing load of circular foundations on a layer of sand of limited thickness by the ANN tool. Momeni*et al.*[42] used ANN and the adaptive neuro-fuzzy inference system (ANFIS) tools to predict the bearing capacity of a thin-walled foundation, considering the geometric parameters of the footing and the geotechnical parameters of soil as input parameters of the predicted model. The prediction of the bearing capacity of a strip footing in front of a slope was treated by Acharyya and Dey [43] using an ANN model based on the numerical results provided by the FE code Plaxis 2D. Hossein Moayedi and Sajad Hayati [44] studied various artificial intelligence–driven tools such as ANN, GA–ANN, PSO–ANN, ANFIS, general regression neural network (GRNN), and feedforward neural network (FFNN) with the objective to model the bearing load of shallow footing near a slope.

Muhammad Nouman Amjad Raja and Sanjay Kumar Shukla [45] have conducted studies to estimate the settlement of geosynthetic-reinforced soil foundations using evolutionary artificial intelligence techniques based on the combination of evolutionary algorithms, namely, Grey Wolf Optimization (GWO) and ANN. An extreme learning machine model has been proposed for the prediction of geosynthetic-reinforced sandy soil foundations based on a large dataset with actual field and laboratory measurements for the validation of this model [46]. A hybrid intelligent model has been used for the prediction of load-settlement behavior with large-scale geosynthetic-reinforced soil abutments [47]. In addition, Khan*et al.*[48] investigated the viability, development, implementation, and comparison of five artificial intelligence–based learning machine models to estimate the settlement of footing located over a buried

conduit within a soil slope. Furthermore, Bardhan*et al.* [49] presented a comparative analysis of hybrid learning machine models by using 10 swarm intelligence algorithms to estimate the soil compression index of clay based on actual laboratory test data. This problem was also treated by Bardhan*et al.*[50] with the development of a high-performance learning machine model based on the improvement of the Harris hawks optimization (IHHO) algorithm. Moreover, several intelligent models have been used to estimate the bearing capacity ratio (CBR) of the reinforced subgrade soil [51] and [52] . Hasthi*et al.*[53] developed a novel hybrid paradigm based on the combination of ANN and dragonfly optimizer (DFO) to predict the amplitude of footing resting on geocell-reinforced soil bed under vibratory load.

This research paper investigates the influence of the reinforcement parameters on the ultimate bearing capacity of a square footing resting on reinforced sand with geosynthetic, using a scale-laboratory model, and the optimization of these parameters using multiobjective optimization. The design parameters considered in this study are the length of the geosynthetic reinforcement (L), their number (N), embedment of the first reinforcement layer (U), and vertical spacing between layers (X), The responses are the bearing capacity and the cost of installing the reinforcement. Calculations will be applied for both geogrid and geotextile reinforcement to validate this strategy.

A central composite design of experiments for each reinforcement type was first adopted to perform the experimental models with different levels of the designed variables to reach these objectives. The statistical tool analysis of variance (ANOVA) was used to analyze the obtained results. The RSM and the ANN techniques were adopted to predict the mathematical models relating to output responses and input variables. A comparison between these regression models was also performed. Finally, the optimization of the design parameters is achieved by combining the ANN tool and the multiobjective GA.

2 Design of experiments

The design of experiments is an effective tool to reduce the operation time. Thus, the design of experiments can reduce costs through the design process. A full factorial design and ANOVA analysis are generally employed to assess the impact of many input factors on the behavior of the output results. Within the context of the factorial design, several values of input parameters are chosen and varied. Each combination is experimentally realized, and the output values are recorded [54]. For each input parameter, n values are determined; so for the k point, a total of n^k combinations are generated and achieved. For the case of a small number of input parameters, the full factorial design generates a reasonable number of combinations. Nevertheless, as their number increases, experiments resulting from this design are becoming computationally more difficult.

Therefore, only a portion of the total n^k factorial design combinations must be considered because higher-level interactions between the input factors are frequently not relevant, emphasizing the significant effect of each parameter. It is possible to replace the n^k experiments to be realized with only $n^{(k-p)}$ combinations, where n^p is the number of realizations deduced from the initial factorial design [54].

2.1 Fractional design called Box–Behnken design

One of the most prominent techniques for optimization using a quadratic regression model is the Box–Behnken design [55]. Each variable can take three levels in this method, with two of those levels representing the same extreme two factorial points in the full factorial design, while the mean value of each factor represents its third level. The Box–Behnken technique provides efficient designs for problems with less than four parameters, and the numbers of consecutive runs are comparable.

3 Predictive methods

3.1 RSM approach

The RSM is a practical tool to determine mathematical models linking input parameters and output responses [26]. The main idea of the RSM is to approximate the output response using an explicit function of the input variables. The expression of this approximation is given below:

$$g(x) = a_0 + \sum_{i=1}^{n} a_i . x_i + \sum_{i=1}^{n} a_i b_j . x_i x_j + \sum_{i=1}^{n} b_i x_i^2 \qquad (1)$$

where x_i are the input variables ;n the number of input parameters; and a_i, b_i, $a_i b_j$ are coefficients to be determined; and $g(x)$ represents the output response.

Also, b_0 is the intercept of the mathematical model and the coefficients b_1, b_2 ...., b_k and b_{12}, b_{13}, $b_{k\text{-}1}$ are the linear and interaction terms, respectively. $g(x)$ represents the output (bearing capacity).

To check the predicted model's capability and ensure that it provides the best approximation for the treated problem, the normal probability plot must be almost within a straight line. ANOVA is also an efficient tool to determine the factors that primarily influence the response. In addition, the evaluation of the coefficients of determination (R^2) and the adjusted R^2 also indicates the robustness of the predictive model.

3.2 Artificial neural network

The technique of ANN is a computational tool inspired by the neuron performance of the human brain and is able to find a mathematical formulation connecting the inputs data and the output results of a defined problem [56].

This technique has been used to solve complex problems due to its exceptional capacity. It is recommended to use these sorts of tools to approximate the response functions in evaluating complicated processes. ANN can be used in place of polynomial regression models to achieve better accuracy and robustness in resolving nonlinear fitting models [57, 58].To obtain significant results, a user must consider the principal factors: network type, network architecture, and network training parameters [56, 59]. The network was designed by incrementally increasing the number of hidden layers and nodes until a suitable architecture could be found. According to Meddour *et al.* [59] and Kalman and Kwasny [60], the tangent hyperbolic function is employed in the hidden layers of the neural network, in which the use of this function speeds up network training compared to the sigmoidal function [61]. Big data is reserved for network training during the calculation, and the rest is utilized for the validation process.

The back propagation algorithm is used to train the network based on the descending gradient rule. This algorithm minimizes the mean square error (MSE) by introducing the input-output patterns sequentially to update weights every time. The minimization is achieved by adjusting weights from the output to the input layer [59].

To evaluate the fitness and the precision of the ANN obtained model, Ramezani and Afsari [62], Rajendra *et al.*[63], and, Garcia-Gimeno *et al.*[64]suggested four indicators, namely coefficient of determination(R^2), root mean square error (RMSE), mean absolute error (MAE) and model predictive error (MPE) and, which are defined as follows:

$$R^2 = \frac{\sum_{i=1}^{n}(y_{i,p}-y_{i,e})}{\sum_{i=1}^{n}(y_{i,p}-y_{average})^2} \quad (2)$$

$$RMSE = \frac{\sqrt{\sum_{i=1}^{n}(y_{i,e}-y_{i,p})2}}{n} \quad (3)$$

$$MAE\ \frac{1}{n}\sum_{i=1}^{n}\left|(y_{i,e}-y_{i,p})\right| \quad (4)$$

$$MPE\ (\%) = \frac{100}{n}\sum_{i=1}^{n}\left|\frac{(y_{i,e}-y_{i,p})}{y_{i,p}}\right| \quad (5)$$

where: n is the number of experiments; $y_{i,e}$, $y_{i,p}$ are the experimental and the predicted values of the ith experiment, respectively; and $y_{average}$ is the average value of experimental results.

The first step to obtain an ANN model is the selection of an appropriate architecture network. The objective is to construct a predicted ANN model by minimizing the model size and errors used during the training and validation [65]. In this study and in all cases, the learning rate adopted is 0.01. Moreover, to select the optimum number of neurons in each hidden layer, proceed by the iterations number variation until a high value of R^2 with a lower value of RMSE parameter is obtained.

4 Experimental model

4.1 Model box

Experimental tests were conducted in a scale model built in the laboratory, constituting of a wooden box whose walls were 20 mm thick. The front wall was made of 12 mm-thick transparent glass (Figure 1). The internal dimensions of the box were 1300 mm × 600 mm in plan and had a depth of 650 mm (Figure 2). The box was supported by a metal table directly fixed in the lab soil by pins (Figure 1). The table was firmly set in a steel frame that supported the system loading via a horizontal steel standard beam. The latter consisted of a manual hydraulic jack with a capacity of 100 kN equipped with a force reading manometer.

Figure 1: View of the laboratory-scale model.

4.2 Model footing

The footing was modeled by square rigid steel with a width of 100 mm and a thickness of 15 mm. A thin layer of sand was glued with epoxy glue on the footing base to ensure a certain roughness during tests.

4.3 Testing material

Natural siliceous sand was used in this research work, with a nominal maximum particle size of 4 mm; it was extracted from the Oum Ali deposit located in Tebessa province (north-eastern Algeria). The specific gravity and fineness modulus of this sand were found to be 2.56 and 2.36, respectively.

Figure 3 presents the grain-size curve of the used sand. According to the United Soil Classification System, this sand is classified as poorly graded sand (SP). The values of effective sizes (D_{10}), (D_{30}) and (D_{60}) are 0.19, 0.30, and 0.45, respectively, while the uniformity coefficient (C_u)=2.368 and the coefficient of curvature (C_c)=1.053. According to the American Society for Testing and Materials (ASTM) standard, the minimum and the maximum dry densities were found to be ρ_{dmin}=1.606 kN/m^3 and ρ_{dmax}=1.867 kN/m^3 respectively.

4.4 Reinforcement elements

Two types of reinforcement, manufactured by the Algerian company Afitex Algeria were used for this study, as shown in Figure 4. The first type of geogrid was Afitex RTE 35-35-40, which was made of high-density polyethylene with an aperture size of 40 × 40 mm. The final tensile strength was 35 kN/m in the two orthogonal directions. The second type of reinforcement was a nonwoven geotextile type AS30, with a mass of 300 g/m^2, made from polypropylene filaments, and its final tensile strength was about 25 kN/m. The properties of the two reinforcements are listed in Table 1.

4.5 Test bed preparation and loading system

A relative density of 35% was adopted for all tests corresponding to loose sand, and a dry density of 1.67 kN/m^3 was obtained on using Equation 6.

$$\rho_d = \frac{\rho_{d\,max} * \rho_{d\,min}}{\rho_{d\,max} - Dr(\rho_{d\,max} - \rho_{d\,min})} \quad (6)$$

The model box was filled with test material in six layers, approximately 100 mm thick for each layer. Light compaction was applied to each layer using a tamper to obtain the appropriate relative density. The upper surface

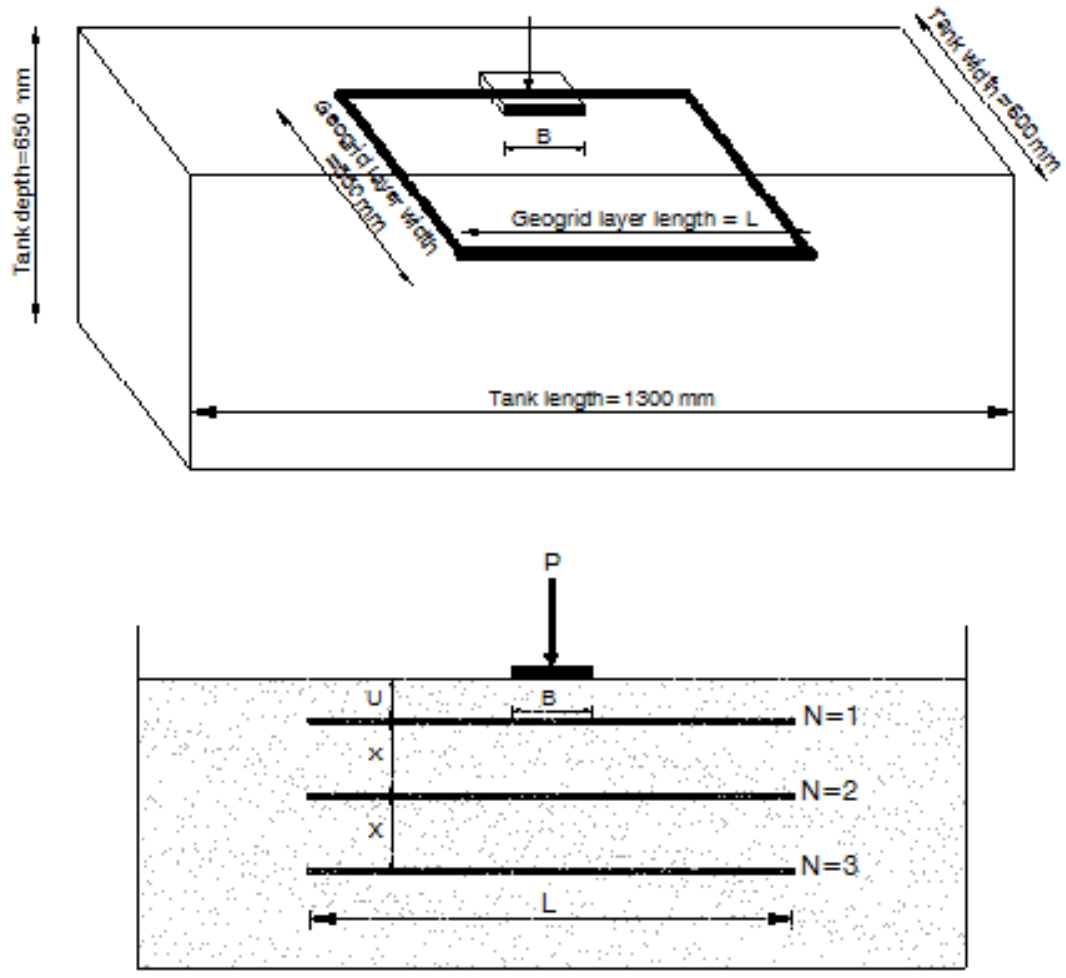

Figure 2: Geometric model and studied parameters of the problem.

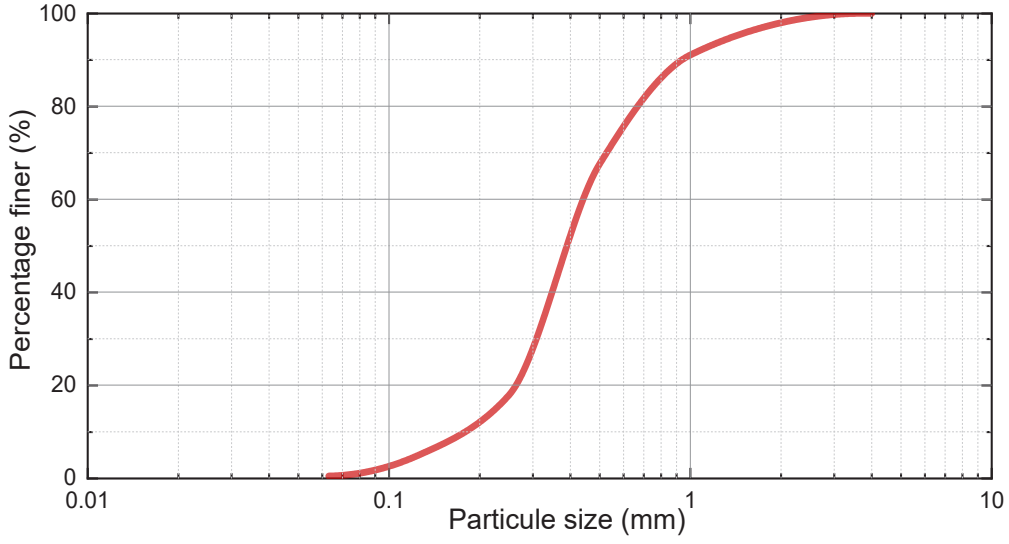

Figure 3: Grain size curve of the testing material.

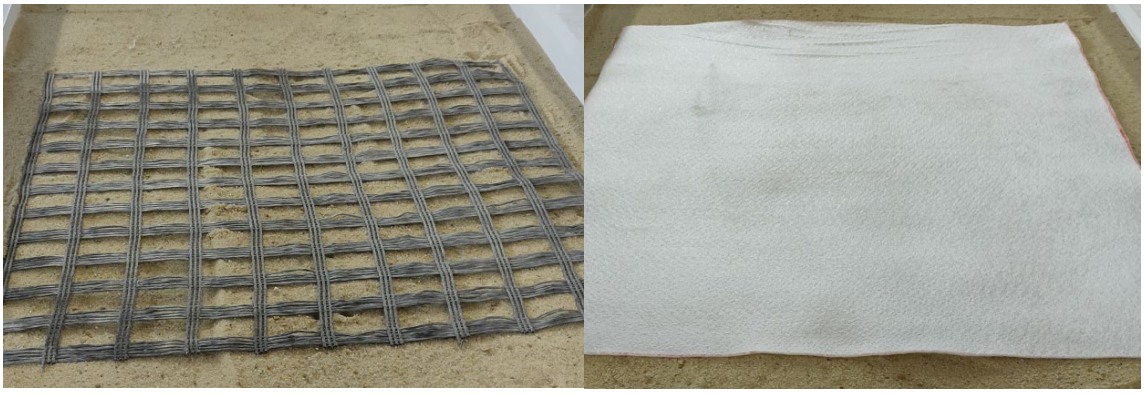

a- Geogrid type AFITEX RTE 35-35-40. b- Geotextile type AS30.

Figure 4: Geosynthetic reinforcements used in this study.

Table 1: Physical and mechanical properties of utilized reinforcement.

Description	GeotextileAS30	Geogrid AFITEX RTE 35-35-40
- Total weight per unit area (g/m²)	300.0	135.0
- Thickness (mm)	1.60	-
- Mesh aperture size (mm)	-	40×40
-Peak tensile strength (kN/m)	25.0	35.0
- Extension at maximum load (%)	75	10
- CBR punching strength (kN)	3.40	-

Table 2: Levels of the input parameters used in the experimental design.

Input parameters	Minimal value	Mean value	Maximal value
Length (L)	5B	7B	9B
Number (N)	1	2	3
Depth of the first layer (U)	0.25B	0.5B	0.75B
Spacing between layers (X)	0.5B	0.75B	1.0B

of the sand was leveled, and special attention was given to obtain the same dry density for all six layers, and therefore a uniform sand bed with a homogeneous unit weight.

The loading system used in this study is shown in Figure 1. It comprises a hydraulic jack with 100 kN capacity, and a loading gauge for reading the applied load, which is attached directly to the reaction frame provided via a horizontal steel beam. The footing settlement was measured using two dial gauges located symmetrically at the ends of the footing. Loading was applied incrementally, and the load increment was restarted after stabilizing the settlement. This loading process was repeated until a settlement of 35 mm of the plate footing was reached. After each test, the test box was imputed and refilled with sand material for the following test at suitable reinforcement configurations.

5 Experimental program

In this study, the Box–Behnken experimental design, with three levels, and four factors, was utilized to investigate the influence of the input variables on the bearing capacity of the reinforced footing. The output result, in this case, is the bearing capacity of the footing q. In contrast, the four input variables are the length of the reinforced layers (L), the number of reinforced layers (N), the depth of the first reinforced layer (U), and the spacing between the layers (X). Their levels according to the footing width B are given in Table 2.

According to the Box-Behnken design with four factors, and three levels, a total of 25 experimental configurations for each reinforcement type as listed in Table 3 will be carried out using the scale model presented above.

6 Results and discussion

Experimental results of 50 tests are presented in terms of the bearing capacity of reinforced sand for the two types of reinforcement as shown in Table 4. These obtained results were evaluated from the stress-settlement curves, in which the settlement (s) of the footing is expressed by the non-dimensional term (s/B), where B is the width footing. The ultimate bearing load is defined as the peak of the load-settlement curve, which marks the collapse of the soil. Footing settlement was obtained as the average of two gauge readings. The bearing capacity of non-reinforced

Table 3: Experimental central composite design L25 of the current study.

Run	Factor 1 L (*B)	Factor 2 N	Factor 3 U (*B)	Factor 4 X (*B)
1	9	1	0.75	1
2	7	2	0.5	0.75
3	5	1	0.25	1
4	9	2	0,5	0.75
5	9	1	0.25	0.5
6	7	2	0.25	0.75
7	9	1	0.75	0.5
8	9	1	0.25	1
9	7	2	0.5	0.5
10	5	3	0.75	1
11	7	2	0.75	0.75
12	7	1	0.5	0.75
13	9	3	0.25	0.5
14	5	3	0.25	1
15	5	1	0.75	1
16	9	3	0.75	0.5
17	5	3	0.75	0.5
18	9	3	0.25	1
19	5	1	0.75	0.5
20	5	1	0.25	0.5
21	5	2	0.5	0.75
22	7	2	0.5	1
23	9	3	0.75	1
24	7	3	0.5	0.75
25	5	3	0.25	0.5

sand was determined, as equal to 75 kPa. The first observations reported from the results in Table 4 show that the reinforcement by geotextile improves the foundation's bearing capacity better than the reinforcement by geogrid. These can be explained by the contact surface offered by the geotextile reinforcement compared to geogrid. The influence of the studied parameters on the bearing capacity of the footing will be discussed in the following sections.

6.1 Effect of reinforcement length

The test results. including the reinforcement length variation (L). are presented in Figures 5 and 6 for both types of reinforcement. It is worth noticing that the bearing capacity increases with increasing reinforcement length at an embedment reinforcement depth of 0.25B; also, the increase generated with geotextile reinforcement was more effective compared to geogrid (Figure 5). However. as shown in Figure 6, from the reinforcement length L = 7.0B. no significant increase in the bearing capacity of the footing was noticed. The lengths 7.0B and 9.0B have almost the same ultimate load in comparison to the size of 5.0B, and this occurs for both types of reinforcement. This finding is consistent with previous studies[66 – 68]. which concluded that the optimal layer length of reinforced sand subjected to axial loads varies between 6.0B and 8.0B. Also, Cicek *et al.* [69], El Sawwaf and Nazir [70], and Abu El-Soud and Belal [71] recommended using a reinforcement length equal to 7.0B for the case of a strip footing reinforced by geogrid to obtain the maximum ultimate bearing capacity.

6.2 Effect of the number of layers

Figures 7 and 8 illustrate the variations of the bearing capacity based on the number of reinforcement layers (N) for both types of reinforcement. In addition. the number of reinforcement varies from one to three layers. It is clear from the load-settlement curves that for the case of N=3, a significant increase in the bearing capacity was observed compared to those with one and two layers. This observation is justified for both cases of reinforcement. It is interesting to note that the influence of the number of layers depends on the depth of the first reinforcement and the vertical spacing between them. These conclusions were also reported by previous studies of reinforced sand supporting strip and square footings and subjected to axial loads [72–74].

6.3 Effect of the embedment of the first reinforcement layer

The model test results for the influence of embedment of the first reinforcement layer are presented in Figure 9 for the case of one layer of reinforcement. Figure 10 for the case of two layers, and Figure 11 for the case of three layers of reinforcement for both geogrid and geotextile reinforcement. The depth U was taken with the values of 0.25B, 0.50B, and 0.75B, with B representing the footing width.

From the obtained results of the different configurations, it is apparent that the height values of

Table 4: Experimental results for the two types of reinforcement.

Run	Factor 1 L (*B)	Factor 2 N	Factor 3 U (*B)	Factor 4 X (*B)	Response 1 $q_{Geogrid}$ (kPa)	Response 2 $q_{Geotextile}$(kPa)
1	9	1	0.75	1	170.0	175.0
2	7	2	0.5	0.75	240.0	270.0
3	5	1	0.25	1	220	240
4	9	2	0.5	0.75	275	280
5	9	1	0.25	0.5	260	275
6	7	2	0.25	0.75	280	350
7	9	1	0.75	0.5	170	210
8	9	1	0.25	1	230	275
9	7	2	0.5	0.5	270	300
10	5	3	0.75	1	160	210
11	7	2	0.75	0.75	165	190
12	7	1	0.5	0.75	180	200
13	9	3	0.25	0.5	360	450
14	5	3	0.25	1	350	485
15	5	1	0.75	1	140	165
16	9	3	0.75	0.5	165	180
17	5	3	0.75	0.5	170	165
18	9	3	0.25	1	300	420
19	5	1	0.75	0.5	140	160
20	5	1	0.25	0.5	220	240
21	5	2	0.5	0.75	245	260
22	7	2	0.5	1	200	240
23	9	3	0.75	1	180	185
24	7	3	0.5	0.75	280	370
25	5	3	0.25	0.5	395	525

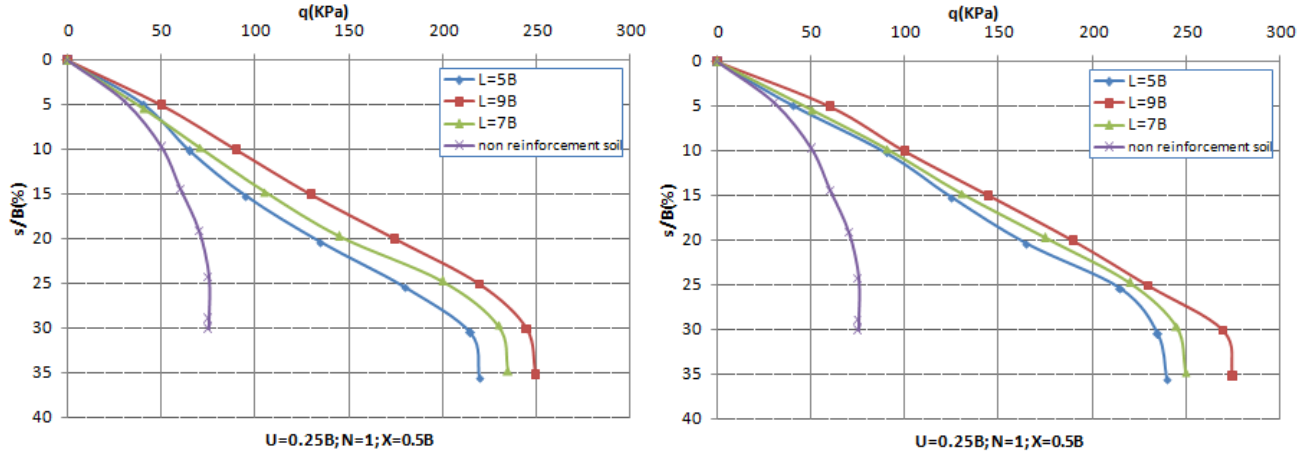

a) Geogrid b) Geotextile

Figure 5: Effect of length on q – s/B relationship (U=0.25B, N=1, X=0.5B).

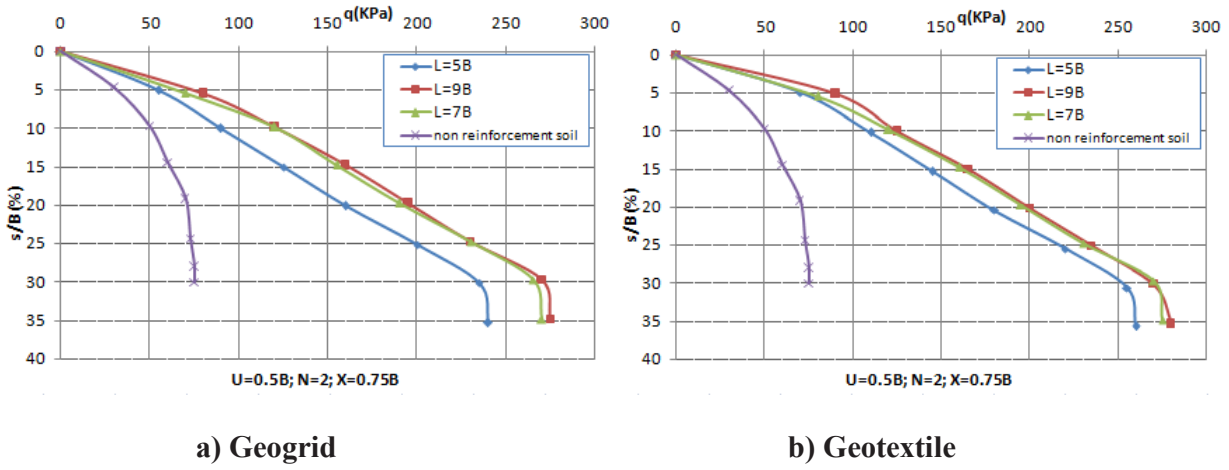

Figure 6: Effect of length on q–s/B relationship (U=0.5B, N=2, X=0.75B).

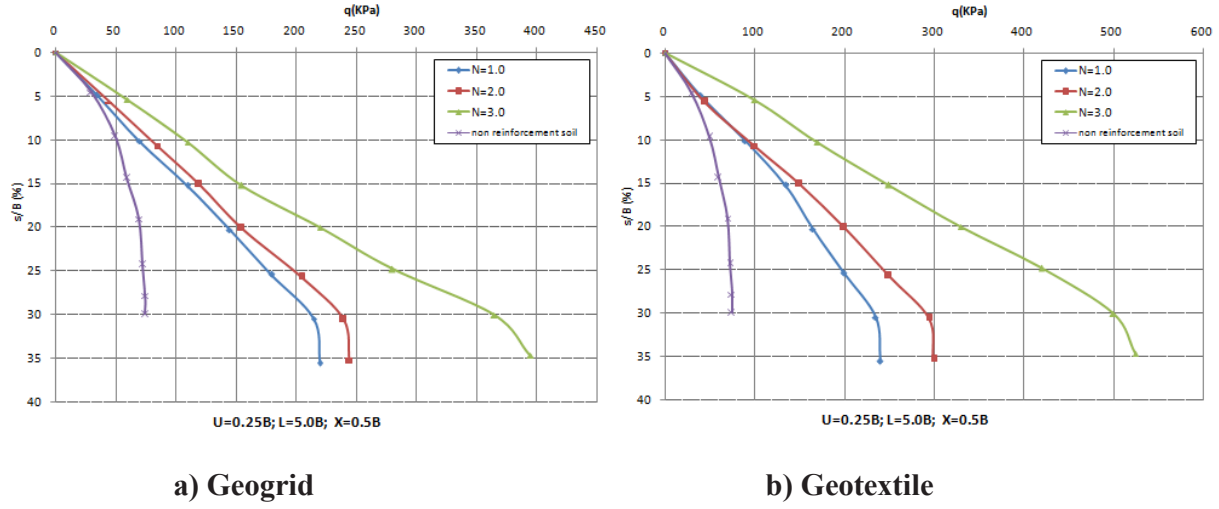

Figure 7: Effect of reinforcement number on q–s/B relationship (U=0.25B, L=5.0B, X=0.5B).

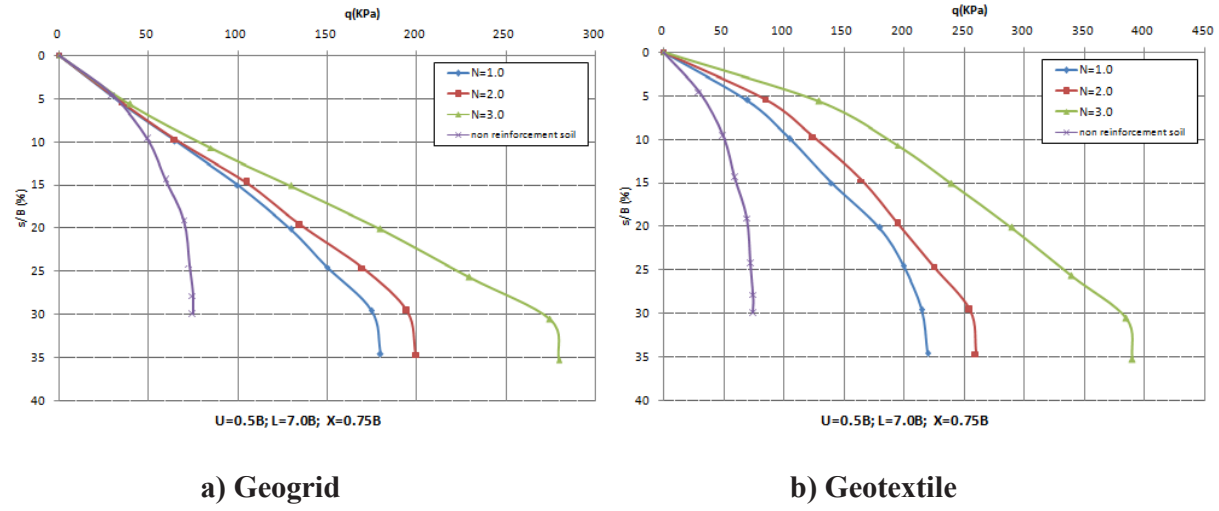

Figure 8: Effect of reinforcement number on q–s/B relationship (U=0.5B, L=7.0B, X=0.75B).

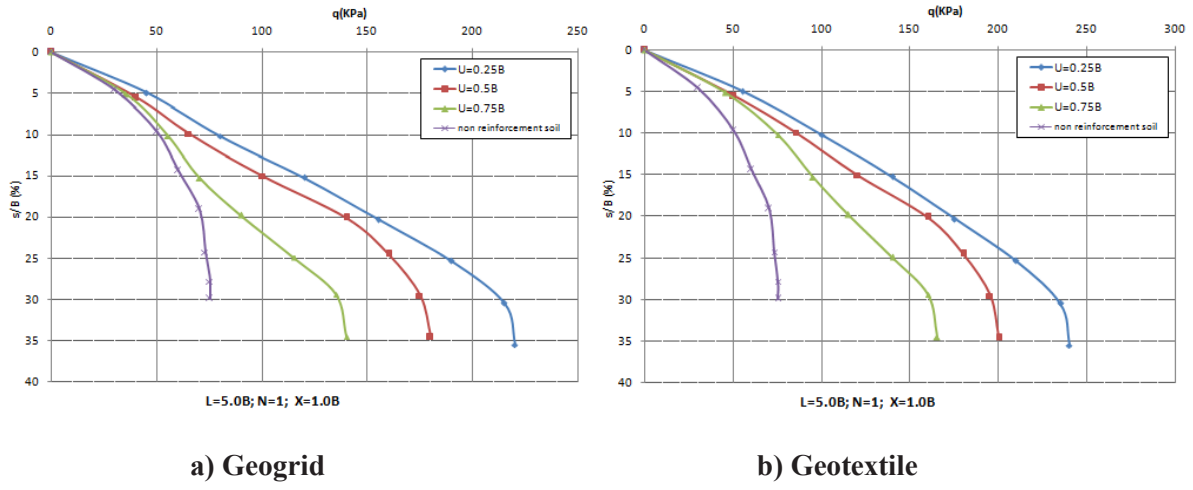

Figure 9: Effect of the depth of the first layer on q–s/B relationship (L=5.0B, N=1, X=1.0B).

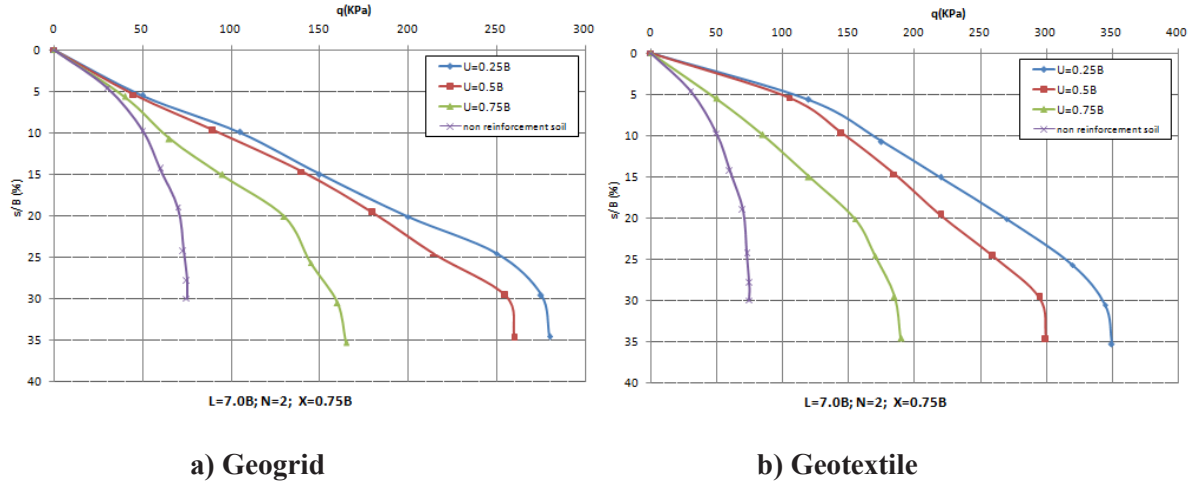

Figure 10: Effect of the depth of the first layer on q–s/B relationship (L=7.0B, N=2, X=0.75B).

the bearing capacity of the footing were acquired at an embedment depth of 0.25B. The depth parameter is directly influenced by the number of reinforcement layers. From Figures 10 and 11, it is worth noticing that the depth of 0.75B loses its influence with the increase in the number of layers. These results are in good agreement with many previous studies dealing with the impact of this parameter for the case of a square and circular footing [75–77].

6.4 Effect of the reinforcement layers spacing

The effect of vertical reinforcement spacing (X) on the bearing capacity was investigated for given values 0.5B, 0.75B, and 1.0B. Figure 12 presents the obtained results based on the load-settlement curve for the two types of reinforcements. It was noticed that the spacing of 0.5B produced the most significant effect.

In addition, the variation of the bearing capacity attributed to the spacing layers variation is less significant than previously studied parameters (U and N). It is worth noting that previous researchers [69, 70, 78] found that the optimum value of the vertical spacing between layers is close to 0.4B.

6.5 Statistical analysis and RSM modeling

6.5.1 ANOVA results

The ANOVA results for the two types of reinforcement used in this study are presented in Tables 5 and 6. with

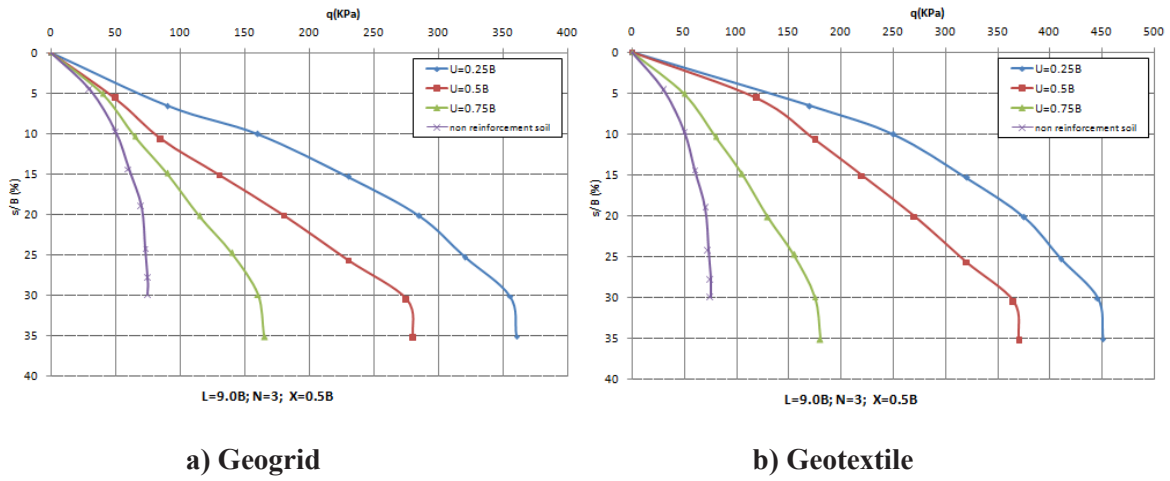

Figure 11: Effect of the depth of the first layer on q–s/B relationship (L=9.0B, N=3, X=0.5B).

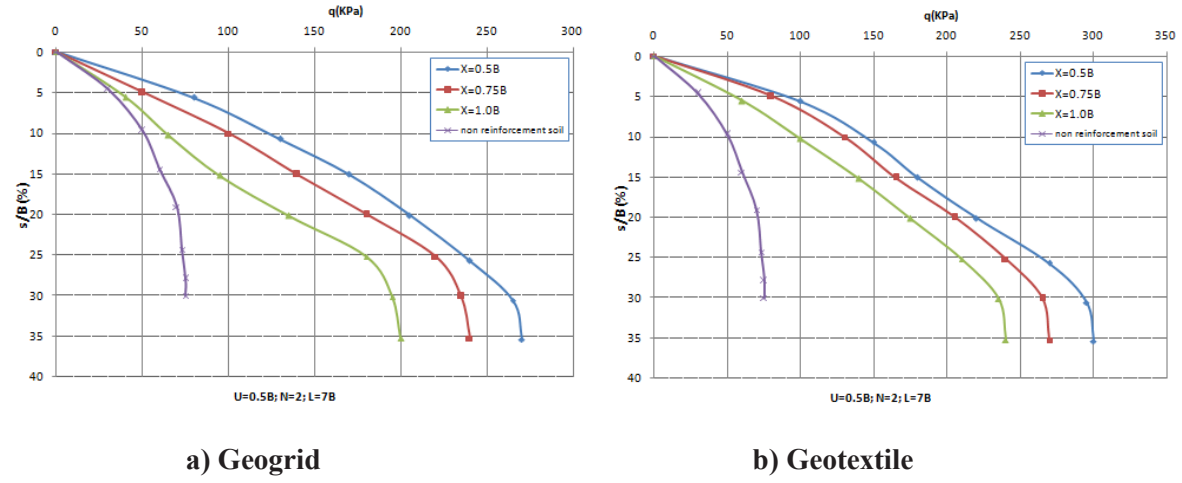

Figure 12: Effect of the spacing reinforcement on q–s/B relationship (U=0.5B, N=2, L=7.0B).

a significance value of α equal to 0.05 (i.e.. the limited confidence interval equals 95%). If the probability (*P*-value) has a low value (≤ 0.05), it can be stated that the approximated models can be assumed as statistically significant and have an acceptable level of accuracy [79]. The ANOVA results for geogrid reinforcement are presented in Table 5; the adopted quadratic model is considered significantly better, with a computed value of R^2 of 0.972 and an Adj-R^2 of 0.947. These values signify that the obtained model can be interpreted as a high correlation between input data and output results. From the results illustrated above, it is clear that the depth of the first geogrid layer (U) is the most significant and influential parameter on the response, with a contribution of 63.762%, followed by the number of the geogrid reinforcement (N), with a contribution of 18.97%. The other two parameters. length of geogrid (L) and spacing between layers (X) have negligible significance with a contribution of 0.234% and 1.381%, respectively. The interaction parameter (L×U) also significantly contributes to the model, with a percentage of 9.485%. However, the rest of the interaction parameters and the quadratic terms have shown a negligible effect.

The adopted quadratic model is considered appropriate. with a coefficient of determination of R^2 of 0.961 and Adj-R^2 of 0.928. As shown in Table 6, the depth of the first reinforcement layer has the most significant influence on the bearing capacity; its contribution is 55.795%. It is followed by the number of layers with a percentage contribution of 23.439%. The increased influence of the interaction term (N×U) with a contribution of 16.082% is also observed; however, the impact of the length (L) and the spacing between layers (X) seems negligible.

Table 5: ANOVA results of the bearing capacity for geogrid reinforcement.

Source	Sum of squares	Df	Mean square	*F* value	*P*-value Prob> *F*	Cont (%)	Remark
Model	1.156E+005	11	10,512.06	40.30	< 0.0001		Significant
L (length of layers)	272.22	1	272.22	1.04	0.3256	0.234	Insignificant
N (number of layers)	22,050.00	1	22,050.00	84.52	< 0.0001	18.970	Significant
U (depth of the first layer)	74,112.50	1	74,112.50	284.10	< 0.0001	63.762	Significant
X (spacing between layers)	1605.56	1	1605.56	6.15	0.0276	1.381	Significant
L*N	2025.00	1	2025.00	7.76	0.0154	1.742	Significant
L*U	756.25	1	756.25	2.90	0.1124	0.651	Insignificant
N*U	11,025.00	1	11,025.00	42.26	< 0.0001	9.485	Significant
U*X	1225.00	1	1225.00	4.70	0.0494	1.054	Significant
L^2	1303.60	1	1303.60	5.00	0.0436	1.122	Significant
U^2	681.69	1	681.69	2.61	0.1300	0.586	Insignificant
X^2	915.48	1	915.48	3.51	0.0837	0.788	Insignificant
Residual	3391.33	13	260.87			0.224	Insignificant
Cor total	1.190E+005	24					

The concluding remarks and conclusions for the geogrid reinforcement can be generalized for the second type of reinforcement; ANOVA results for geotextile are presented in Table 6.

6.5.2 Regression equations

The regression analysis technique is widely applied to model the correlation between input factors and output results and is suitable for modeling and resolving engineering problems. It helps in the determination of a reliable approximation for an appropriate correlation [80]. It is generally approximated by mathematical functions when models are built by performing a set of organized experiments using an orthogonal array of experiments [81]. Based on the use of Design Expert V10 software, the relationships between the input parameters (length (L), number (N), depth of the first layer (U), and spacing between layers (X), and the bearing capacity of the footing for the two types of reinforcement are modeled by quadratic regression models and are presented below equations 7 and 8, with a coefficient of determination R^2 of 97.20% and 96.10%, respectively.

$$q_{geogrid} = 268.428 - 69.850 * L + 126.875 * N + 3.882 * U + 329.920 * X - 5.625 * L * N + 13.750 * L * U - 105.00 * N * U + 140.00 * U * X + 5.441 * L^2 - 251.798 * U^2 - 291.798 * X^2 \quad (7)$$

$$q_{geotextile} = 55.066 + 72.774 * L + 222.083 * N + 203.831 * U - 671.059 * X - 8.750 * L * N + 15.00 * L * U - 205.00 * N * U + 90.00 * U * X - 4.473 * L^2 - 326.331 * U^2 + 393.669 * X^2 \quad (8)$$

6.5.3 Graphical validation of the models

Figure 13 shows the 3D response surfaces for the evolution of the load capacity corresponding to the interaction effects of the input parameters (U×L,U×N, and U×X) in the designed space, based on the regression equations listed above.

Figure 13 a illustrates the evolution of the response based on the variation in the depth of the first layer (U) and the length of the layers (L) variation. It can be observed clearly that the bearing capacity increases with decreasing depth (U). However, the variation rate of (L) has a slight influence on the response. These observations can be applied to the two reinforcements that confirmed the results obtained from ANOVA analysis.

The evolution of the response based on the variation in the depth of the first layer (U) and the number of layers (N) variation is presented in Figure 13 b. As it can be seen from the two types of reinforcement, the response increases with decreasing depth (U) and increasing the number of layers (N).

It is evident that the depth of the first layer (U) rate has a significant influence on the response when compared to the number of layers (N) rate variation, as long as its slope

Table 6: ANOVA results of the bearing capacity for geotextile reinforcement.

Source	Sum of squares	Df	Mean square	*F* value	*P*-value Prob> F	Cont (%)	Remark
Model	2.601E+005	11	23,641.60	28.90	< 0.0001		Significant
L (length of layers)	1.39	1	1.39	1.698E-003	0.9678	0.001	Insignificant
N (number of layers)	61,250.00	1	61,250.00	74.86	< 0.0001	23.439	Significant
U (depth of the first layer)	1.458E+005	1	1.458E+005	178.20	< 0.0001	55.795	Significant
X (spacing between layers)	1422.22	1	1422.22	1.74	0.2101	0.544	Insignificant
L*N	4900.00	1	4900.00	5.99	0.0294	1.875	Significant
L*U	900.00	1	900.00	1.10	0.3134	0.344	Insignificant
N*U	42,025.00	1	42,025.00	51.36	< 0.0001	16.082	Significant
U*X	506.25	1	506.25	0.62	0.4456	0.194	Insignificant
L^2	881.50	1	881.50	1.08	0.3182	0.337	Insignificant
U^2	1144.99	1	1144.99	1.40	0.2580	0.438	Insignificant
X^2	1666.27	1	1666.27	2.04	0.1771	0.638	Insignificant
Residual	10,636.42	13	818.19			0.313	Insignificant
Cor total	2.707E+005	24					

variation is higher than the number of layers (N) slope variation. These observations were in good agreement with the results obtained from ANOVA analysis, as shown in Tables 5 and 6. Consequently, higher rates of response are obtained by using smaller values of (U) with higher rates of (N).

Figure 13 c shows the 3D response surfaces of the response based on the variation in depth (U) and spacing between layers (X) variation. It can be seen that for the two types of reinforcement, the bearing capacity increases with decreasing the two parameters (U) and (X). The slope variation of the response according to the depth (U) rate is higher than the spacing (X) rate. These remarks agree with the results from the ANOVA analysis as mentioned above.

6.6 ANN modeling

6.6.1 ANN modeling of the bearing load of footing with geogrid reinforcement

Figure 14 illustrates the adequate ANN architecture of the bearing capacity (q) model (4-8-1) for the foundation reinforced by geogrid. represented by four input nodes (L, N, U, and X) with height nodes in the hidden layer and one node for the output layer (bearing capacity). This final architecture is obtained after an optimal number of 100 iterations.

The mathematical model for the above ANN architecture is presented by equation 9. This model results from the product of hidden layers of the height neurons to a linear function.

$$q=-69.473xH_1+215.834xH_2+54.268xH_3-55.959xH_4-68.668xH_5+146.937xH_6-2.331xH_7+133.836xH_8+329.913 \quad (9)$$

where H_1–H_8 are the outputs of each neuron of the hidden layer and are expressed as follows:

$$\begin{aligned}
H_1&=\tanh(0.5x(0.123xL+0.487xN+5.247xU-0.487xX-2.981))\\
H_2&=\tanh(0.5x(0.156xL+0.056xN-2.558xU-1.000xX-1.839))\\
H_3&=\tanh(0.5x(0.383xL-1.638xN+2.831xU+0.714xX-1.829))\\
H_4&=\tanh(0.5x(-0.768xL-1.292xN+9.177xU-4.173xX+5.945))\\
H_5&=\tanh(0.5x(0.091xL+3.308xN-5.908xU+7.514xX-11.140))\\
H_6&=\tanh(0.5x(-0.386xL+1.343xN-3.795xU+1.118xX+0.113))\\
H_7&=\tanh(0.5x(1.092xL+0.357xN+2.585xU+5.875xX-14.242))\\
H_8&=\tanh(0.5x(-0.173xL+1.579xN+9.080xU-5.964xX+0.047))
\end{aligned} \quad (10)$$

Predicted and observed results for training and validation cases are presented in Figure 15.

As shown in Figure 15, it is crucial to note that the intersection between experimental and predicted values of the bearing capacity (q) is close to the median line for both cases. The coefficient of determination R^2 is 0.9991 for the training case and 1.0 for the validation case; the value

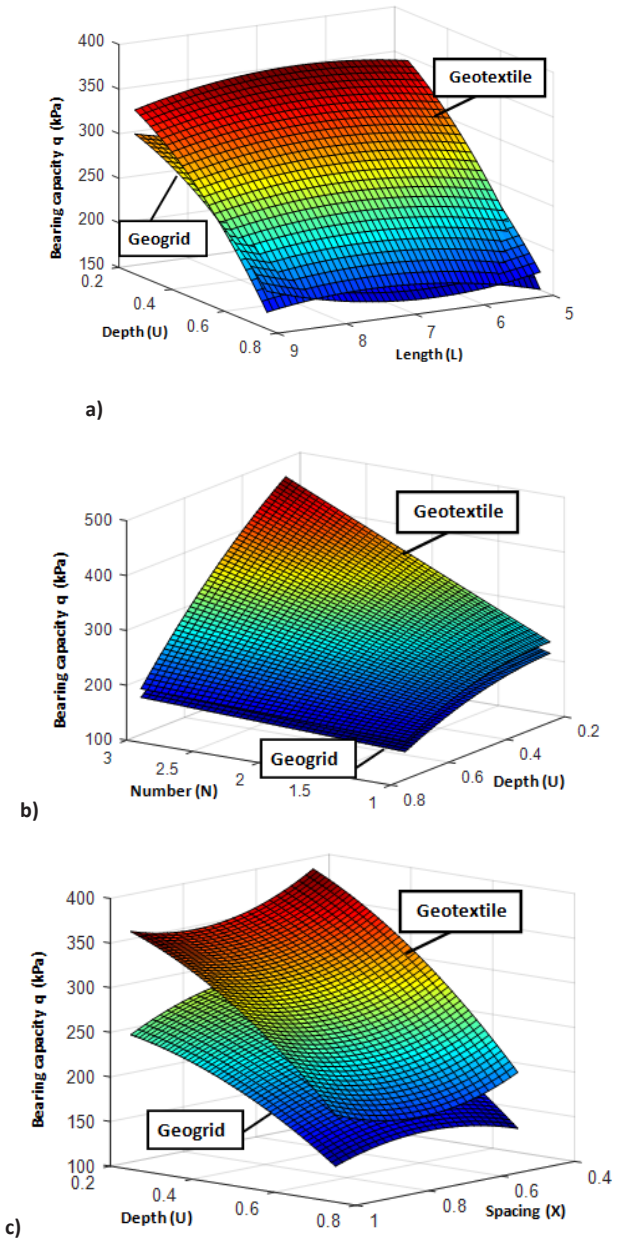

Figure 13: Effect of geometric parameters on the bearing capacity for the three soils.

of RMES is 2.0495 and 0.0142 for both cases. respectively. These revealed the robustness of the fitted mathematical model.

6.6.2 ANN modeling of the bearing load of footing reinforced with geotextile

The ANN architecture for the footing reinforced by geotextile is illustrated in Figure 16, it consists of four input nodes, a hidden layer with eight nodes, and one

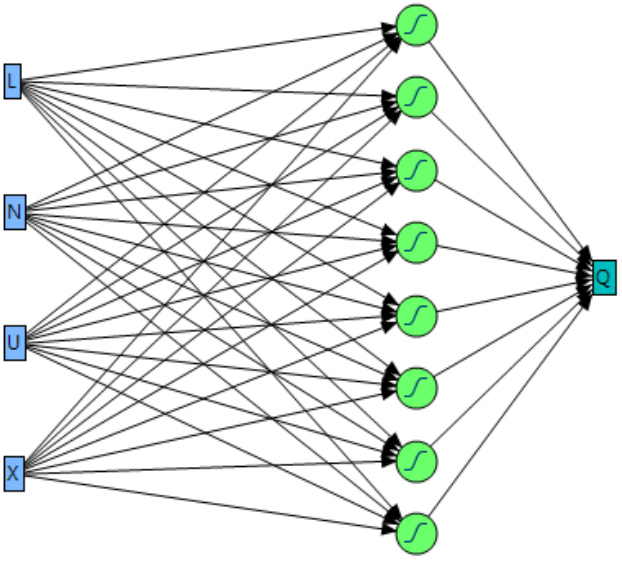

Figure 14: ANN architecture (4 -8 -1) for bearing capacity q.

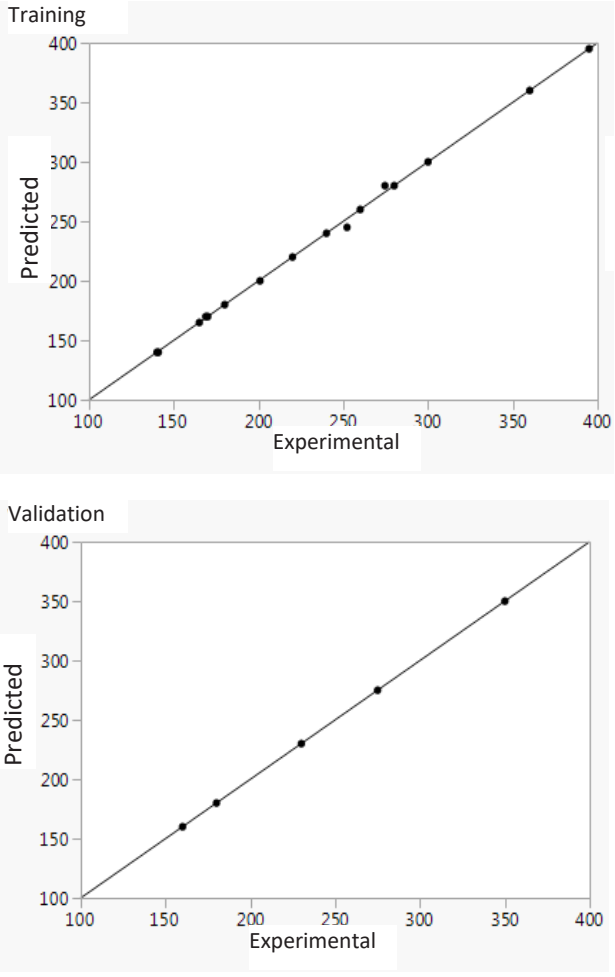

Figure 15: Predicted versus experimental values for bearing capacity q.

output node (4-8-1). This obtained configuration was validated after a number of 100 iterations.

The predicted mathematical model for this case is presented by equation 11. The model results from the product of hidden layers of the height neurons to a linear function.

$$q=99.643xH_1+84.155xH_2-35.755xH_3+25.536xH_4+141.912xH_5-49.333xH_6-74.838xH_7+135.006xH_8+202.524 \quad (11)$$

where H_1–H_8 are the outputs of each neuron of the hidden layer and are expressed as follows:

$$\begin{aligned}
H_1&=\tanh(0.5x(1.218xL+1.489xN-6.070xU+1.038xX-7.934))\\
H_2&=\tanh(0.5x(-0.604xL-0.287xN-1.304xU+3.376xX+1.749))\\
H_3&=\tanh(0.5x(-0.153xL-0.786xN+3.747xU-7.579xX+5.608))\\
H_4&=\tanh(0.5x(+0.301xL-1.828xN-9.566xU-12.053xX+13.420))\\
H_5&=\tanh(0.5x(0.347xL+0.702xN+1.970xU-1.471xX-3.102))\\
H_6&=\tanh(0.5x(0.191xL-3.599xN+10.837xU+3.452xX+0.621))\\
H_7&=\tanh(0.5x(2.681xL+0.352xN-6.416xU+10.053xX-23.192))\\
H_8&=\tanh(0.5x(-0.020xL-1.004xN-7.198xU-0.214xX+8.290))
\end{aligned} \quad (12)$$

Figure 17 shows the experimental and predicted results for the two cases (training and validation). For both cases, it is essential to notice that the observed and the fitted values are closest to the straight line.

The coefficient of determination R^2 is 0.9998 for the training case and 1.0 for the validation case; the value of RMES is 1.038 and 0.0233 for both cases, respectively. These also revealed the robustness of the fitted mathematical model.

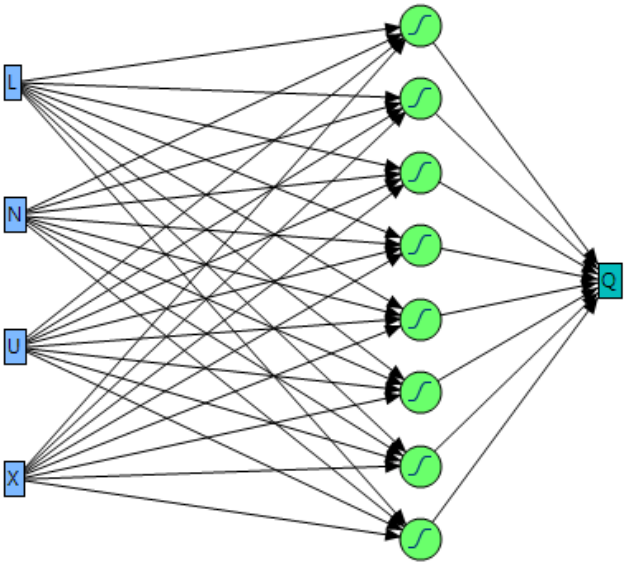

Figure 16: ANN architecture (4 -8 -1) for the bearing capacity q.

6.6.3 Sensitivity analysis of the ANN model

To evaluate the influence of each input parameter on the bearing capacity model, developed by the ANN, a sensitivity analysis was adopted by using the cosine amplitude method (CAM). This method has been developed to calculate the strength of the relationship between two parameters [51].

In this method, all the data pairs (each of the input parameter and the target parameter) would form an X array. with:

$$\text{X array. with: } X_i = \{x_1.x_2.x_3.\ldots\ldots x_m\}, \quad (13)$$

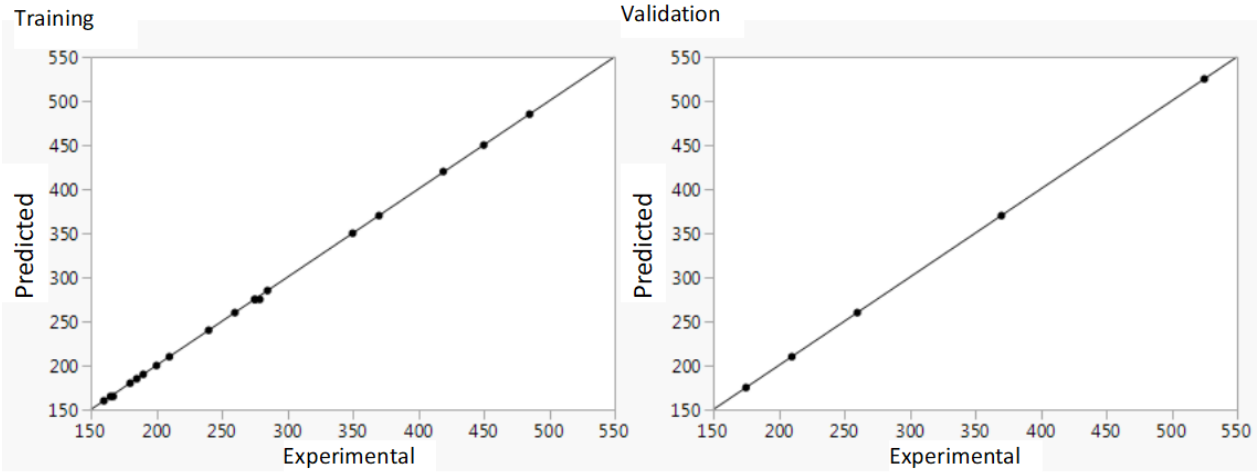

Figure 17: Predicted versus experimental values for the bearing capacity q.

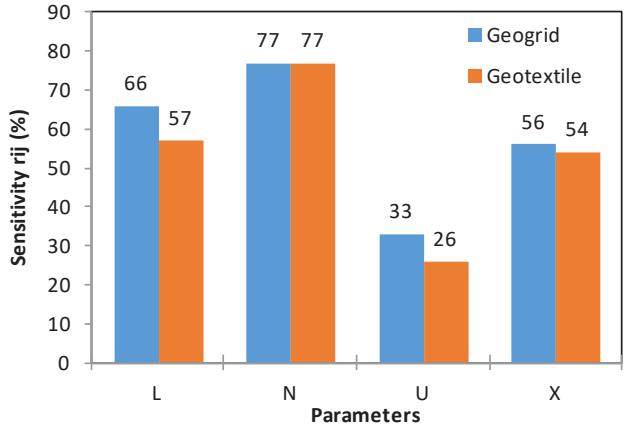

Figure 18: Results of sensitivity analysis using CAM.

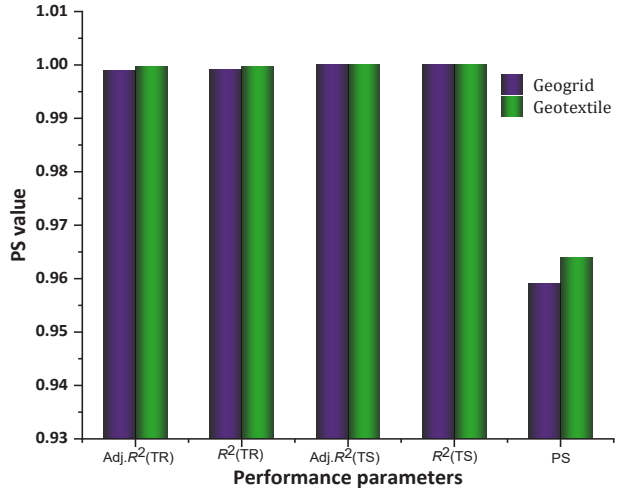

Figure 19: Bar plot of PS values.

were each element x_i of equation (12) is a vector with length m, and it is defined as

$$X_i = \{x_{i1}.x_{i2}.x_{i3}.\ldots\ldots x_{im}\} \tag{14}$$

The correlation strength r_{ij} between the input factors x_i and the target x_j can be expressed as follows [51]:

$$r_{ij} = \frac{\sum_{k=1}^{m} x_{ik}x_{jk}}{\sqrt{\sum_{k=1}^{m} x_{ik}^2 \sum_{k=1}^{m} x_{jk}^2}} \quad . \quad 0 \le r_{ij} \le 1 \tag{15}$$

Results of sensitivity analysis for the ANN model for both types of reinforcement are presented in Figure 18. In this figure, it is worth noticing that all the input parameters have a significant contribution in the formulation of the model in both cases. The parameter variation range is between 33% and 77% for georgid reinforcement. and between 26% and 77% for geotextile reinforcement.

6.6.4 Performance strength of the ANN model

For the analysis of the strength performance of the obtained ANN model, the performance strength index (PS) was used and it can be defined as follows:

$$PS = \frac{(\text{Adj.}R^2)_{total} + (0.01\text{VAF})_{total} - (\text{RMSE})_{total}}{\left(\frac{\text{Adj.}R^2}{R^2}\right)_{training} + \left(\frac{\text{Adj.}R^2}{R^2}\right)_{testing}} \tag{16}$$

The PS index can provide the strength of performance of a predictive model using the values of Adj.R^2 and R^2 for both training and testing datasets along with the values adjustement factor (VAF) and RMSE for the total dataset. The ideal value of PS is 1 [82]. The VAF is defined by equation 17 as shown below:

$$\text{VAF}\ (\%) = \left[1 - \frac{\text{var}((y_{i.e} - y_{i.p})}{\text{var}(y_{i.e})}\right] x100 \tag{17}$$

By using the expression shown in equation 16, the values of PS obtained from the predicted models for both types of reinforcement are shown in Figure 19, with a PS index R^2 of 0.959 for the geogrid reinforcement and 0.964 for the other type of reinforcement. The obtained PS index revealed the robustness of the fitted ANN models.

Another indicator of the performance of the ANN models is called the objective function (OBJ). It determines the accuracy of the fitted models in training and testing data sets. The lower value of this indicator represents more accuracy and vice versa [51]. This expression is based on RMSE, R^2, and MAE coefficients and can be estimated as

$$OBJ = \left(\frac{N_{o.tr} - N_{o.ts}}{N_{o.tr} + N_{o.ts}}\right) x \frac{\text{RMSE}_{tr} + \text{MAE}_{tr}}{R_{tr}^2 + 1} + \left(\frac{2N_{o.ts}}{N_{o.tr} + N_{o.ts}}\right) x \frac{\text{RMSE}_{ts} + \text{MAE}_{ts}}{R_{ts}^2 + 1} \tag{18}$$

where subscripts tr and ts represent training and testing data, respectively.

Based on the calculated values of the OBJ function (OBJ = 0.642 for the geogrid reinforcement model and OBJ = 0.211 for the geotextile reinforcement model), it can be concluded that the obtained ANN models have reliable accuracy and confirm the previous comparison criteria.

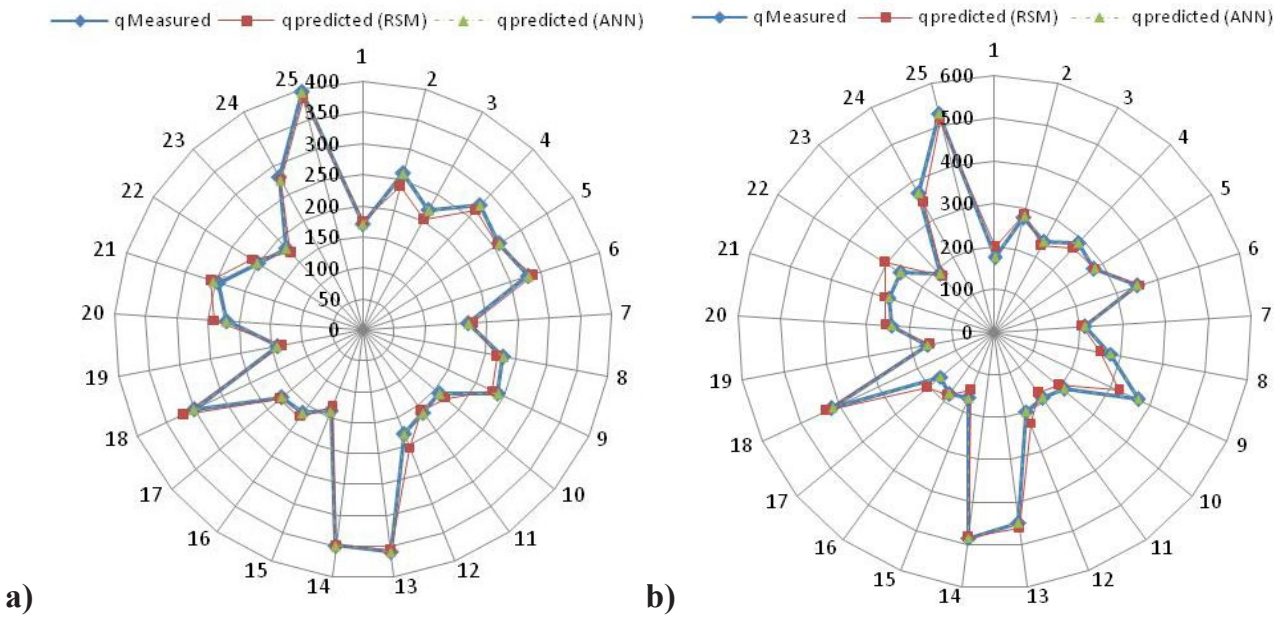

Figure 20: Comparison between predicted and experimental values for q with RSM and ANN models (a- geogrid reinforcement. b- geotextile reinforcement).

Table 7: Comparison between RSM and ANN models.

Type of reinforcement	RSM			ANN		
	R^2	RMSE	MPE (%)	R^2	RMSE	MPE (%)
Geogrid	0.972	0.3595	0.7215	0.9991	0.057	0.0414
Geotextile	0.961	0.6366	1.027	0.9998	0.0286	0.021

6.7 Comparison of RSM and ANN models

A comparison between the RSM and ANN methods was made to determine the accuracy of the predictive models. In this step, some comparisons were required to evaluate the difference between experimental results and predicted values obtained by RSM and ANN models. Terms of comparison for the two predicted models are the highest coefficient of determination R^2 and low values of RMSE and mean prediction error (MPE). The differences between experimental and predicted responses using RSM and ANN models for both geogrid and geotextile reinforcement are presented in Figure 20. It is evident from this figure that the experimental and ANN predicted values are very close to each other compared to RSM predicted values.

Indeed, coefficients R^2 obtained by RSM models are 0.972 for geogrid reinforcement and 0.961for the second reinforcement type, and their corresponding values, obtained using ANN models are 0.9991 and 0.9998, respectively (see Table 7). In addition, the RMSE and MPE estimated values based on ANN fitted models are more accurate than those of RSM models. The RMSE and MPE calculated values are 0.057% and 0.0414%, respectively, for the ANN model and their values for the RSM model are 0.3595% and 0.7215%, respectively, for geogrid reinforcement. Similar observations and conclusions can be made for geotextile reinforcement (Table 7). As a result and based on the above statements, the ANN models will be adopted for the optimization process later.

6.8 Estimation of the reinforcement cost

To better estimate the cost of reinforcement, costs of material and installation are taken into consideration. The material cost noted, cost (M), is controlled by the number (N) and the length (L) of the layer reinforcement. In contrast. the installation cost noted cost (I) would depend on the depth of the first reinforcement layer (U) and the vertical spacing between layers (X). The total cost of the reinforcements is estimated as follows:

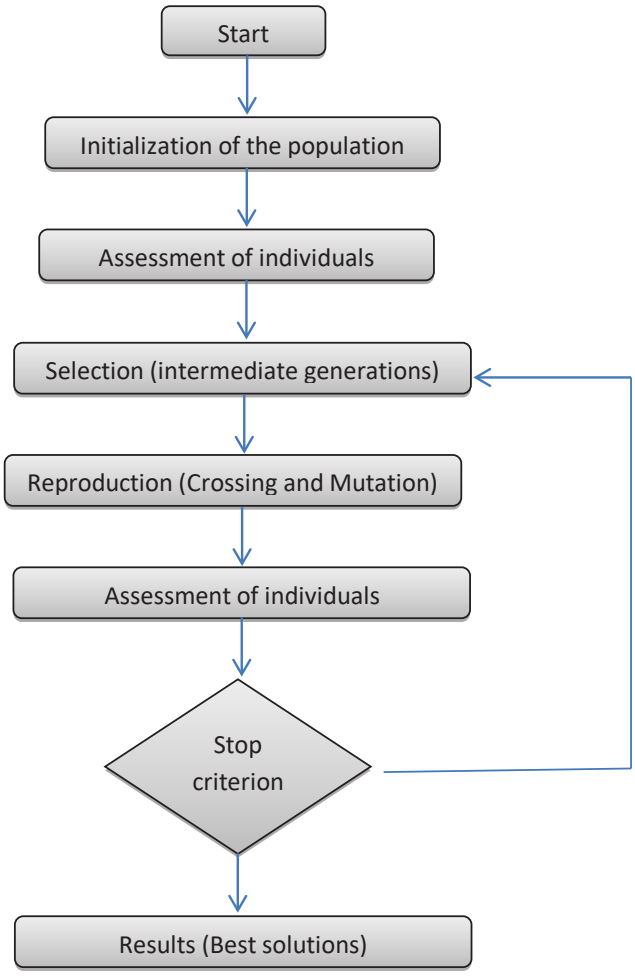

Figure 21: Diagram of the genetic algorithm.

$$\text{Total Cost}=\text{Cost (M)}+\text{Cost (I)} \tag{19}$$

$$\text{Cost (M)}=\text{LxN.and Cost (I)}=\text{U}+\text{X}*(\text{N-1}) \tag{20}$$

The total cost can be estimated using the equation

$$\text{Total Cost}=\text{LxN}+\text{U}+\text{X}*(\text{N-1}) \tag{21}$$

6.9 Optimization using multiobjective GA

The multi-objective optimization aims to find a compromise between several criteria and compute the values of the input parameters that can be brought to the optimal values of the response outputs [83]. taking into account some requirements simultaneously. Many optimization methods are available for solving both constrained and unconstrained problems. GAs are the most widely used optimization methods. Primarily, creating an arbitrarily initial population named chromosomes will be considered an initial solution, whose principal performance is evaluating the fitness function. Then. according to the obtained results, several pairs among these potential solutions are generated using evolutionary techniques such as selection, crossing, and mutation. The procedure of the resolution system may be repeated until the best solution is achieved [84] (Figure21).

The present work performs a combination of the maximization of the bearing capacity of a shallow footing (q) and, at the same time, minimization of the construction cost. It was performed with four input variables (L, N, U and X). The length (L) varied between 5.0B and 9.0B, the number of reinforcement layers between one and three, the depth of the first layer between 0.25B and 0.75B and the vertical spacing between 0.5B and 1.0B. The multiobjective GA tool is used based on the mathematical model formulated by the ANN method. The constraints used in the present optimization are displayed in Table 8.

Creating a program file containing fitness functions was performed using Matlab software. The characteristics of the multiobjective GA, such as population. crossover distribution index, mutation distribution index. crossover probability, and mutation probability, were set using the GA toolbox implemented in Matlab software as presented in Table 9.

Table 10 presents the obtained results according to GA optimization for the reinforcement parameters and the responses for the two types of reinforcement.

7 Conclusions

The present study investigated evaluation of the bearing capacity of a square footing resting on sandy soil improved by geosynthetic reinforcements on the one hand and the optimization of the influenced reinforced parameters using a laboratory scale model on the other hand. The work considered a multi-objective problem considering two conflicting responses: the bearing capacity and cost installation of the geosynthetic. Both the RSM and ANN tools and the multiobjective optimization GA were used to model and optimize the problem. From this study. the following conclusions can be drawn:

- A significant increase in the bearing capacity of reinforced sand was recorded compared to that related to the non-reinforced case.
- The improvement of the bearing capacity generated by geotextile was more significant than that generated by geogrid. This can be explained by the importance of

Table 8: Optimization conditions.

Parameters		Objective	Lower limit	Upper limit
L (B)		Is in range	5.0	9.0
N		Is in range	1	3
U (B)		Is in range	0.25	0.75
X(B)		Is in range	0.5	1.0
q (kPa)	Geogrid	Maximization	140.0	395.0
	Geotextile		160.0	525.0
Cost (B)		Minimization	5.25	29.75

Table 9: GA parameters.

Parameters	Values
Number of variables	4
Size of population	100
Selection function	Stochastic uniform
Crossover fraction	0.8
Mutation probability	0.2
Number of generations	100

Table 10: Optimization results.

Reinforcement	L (B)	N	U(B)	X(B)	q (kPa)	Cost (B)
Geogrid						
	5.00	2	0.25	0.50	324.65	10.76
Geotextile						
	5.00	2	0.25	0.50	374.44	10.85

the contact surface with the soil offered by geotextile compared to the geogrid.

- The increase in bearing capacity become more evident as the depth of the first layer reinforcement decreased. This conclusion was confirmed by the ANOVA for the two types of reinforcement. It indicated that the depth (U) had the most significant influence on the predicted models.
- The optimum value for the depth of the first reinforcement layer (U) was estimated to be 0.25B, and the length of reinforcement layers (L) was found to be 7.0B (with B as the footing width). The bearing capacity reaches its maximum value for a number of reinforcement layers (N) equal to three, and the optimum vertical spacing between layers (X) was found to be 0.5B.
- The above experimental findings were confirmed using the proposed method based on multi-objective optimization.
- The ANN method provided more accuracy for predicted models than the RSM method.
- The coupling of the ANN method and the multiobjective optimization GA was found to be a very efficient tool for predicting the conflicting multiobjective problems.

Finally, it is worth noticing that the obtained results of this study are specific to a square footing with a 10 cm width and for loose sand with a relative density of 35%. The effect of other parameters. such as the density of used sand. footing dimensions and types, scale effect, and other, has not been considered in this work.

Conflict of Interest: The authors declare no conflicts of interest regarding this manuscript. and there is no significant financial support for this work that could have influenced its outcome.

References

[1] P. K. Kolay, S. Kumar, and D. Tiwari(2013).Improvement of Bearing Capacity of Shallow Foundation on Geogrid Reinforced Silty Clay and Sand.Journal of Construction Engineering Volume 2013, Article ID 293809, 10 pages.http://dx.doi.org/10.1155/2013/293809.

[2] Abu El-Soud, S., Belal, A.M (2018).Bearing capacity of rigid shallow footing on geogrid-reinforced fine sand—experimental modeling.*Arab J Geosci***11,** 247 (2018). https://doi.org/10.1007/s12517-018-3597-0.

[3] J. Binquet and K. L. Lee, (1975)."Bearing capacity tests on reinforced earth slabs,"*Journal of Geotechnical Engineering Division*, vol. 101, no. 12, pp. 1241–1255, 1975.

[4] J. Binquet and K. L. Lee, (1975)."Bearing capacity analysis of reinforced earth slabs,"*Journal of Geotechnical Engineering Division*, vol. 101, no. 12, pp. 1257–1276, 1975.

[5] V. A. Guido, D. K. Chang, and M. A. Sweeney, (1986). "Comparison of geogrid and geotextile reinforced earth slabs,"*Canadian Geotechnical Journal*, vol. 23, no. 4, pp. 435–440, 1986.

[6] J. P. Sakti and B. M. Das, (1987). "Model tests for strip foundation on clay reinforced with geotextile layers,"*Transportation Research Record*, no. 1153, pp. 40–45, 1987.

[7] P. K. Basudhar, S. Saha, and K. Deb, (2007)."Circular footings resting on geotextile-reinforced sand bed,"*Geotextiles and Geomembranes*, vol. 25, no. 6, pp. 377–384, 2007.

[8] G. W. E. Milligan, R. J. Fannin, and D. M. Farrar, (1986). "Model and full-scale tests on granular layers reinforced with a geogrid," in *Proceedings of the 3rd International Conference on Geotextiles*, vol. 1, pp. 61–66, Vienna, Austria, 1986.

[9] K. H. Khing, B. M. Das, V. K. Puri, S. C. Yen, and E. E. Cook, (1994).“Foundation on strong sand underlain by weak clay withgeogrid at the interface,”*Geotextiles and Geomembranes*, vol. 13, no. 3, pp. 199–206, 1994.

[10] B. M. Das, K. H. Khing, and E. C. Shin, (1998).“Stabilization of weak clay with strong sand and geogrid at sand-clay interface,”*Transportation Research Record*, no. 1611, pp. 55–62, 1998.

[11] E. C. Shin, B. M. Das, V. K. Puri, S. C. Yen, and E. E. Cook, (1993). “Bearing capacity of strip foundation on geogrid-reinforced clay,”*Geotechnical Testing Journal*, vol. 17, no. 4, pp. 535–541, 1993.

[12]C. R. Patra, B. M. Das, and C. Atalar, 2005).“Bearing capacity of embedded strip foundation on geogrid-reinforced sand,” *Geotextiles and Geomembranes*, vol. 23, no. 5, pp. 454–462, 2005.

[13] B. R. Phanikumar, R. Prasad, and A. Singh, 2009).“Compressive load response of geogrid-reinforced fine, medium and coarse sands,”*Geotextiles and Geomembranes*, vol. 27, no. 3, pp. 183–186, 2009.

[14] Y. L. Dong, J. Han, and X.-H.Bai, (2010).”Bearing capacities of geogridreinforced sand bases under static loading,” in *Proceedings of GeoShanghai International Conference: Ground Improvement and Geosynthetics*, pp. 275–281, June 2010.

[15]R. J. Fragaszy and E. Lawton, (1984).”Bearing capacity of reinforced sand subgrades,”*Journal of Geotechnical Engineering*, vol. 110, no. 10, pp. 1500–1507, 1984.

[16] C.-C. Huang and F. Tatsuoka, (1990).”Bearing capacity of reinforced horizontal sandy ground,”*Geotextiles and Geomembranes*, vol. 9, no. 1, pp. 51–82, 1990.

[17] J. O. Akinmusuru and J. A. Akinbolade, (1981).”Stability of loaded footings on reinforced soil,”*Journal of the Geotechnical Engineering Division*, vol. 107, no. 6, pp. 819–827, 1981.

[18] T. Yetimoglu, M. Inanir, and O. E. Inanir, (2005).“A study on bearing capacity of randomly distributed fiber-reinforced sand fills overlying soft clay,”*Geotextiles and Geomembranes*, vol. 23, no. 2, pp. 174–183, 2005.

[19] S. K. Dash, N. R. Krishnaswamy, and K. Rajagopal, (2001).”Bearing capacity of strip footings supported on geocell-reinforced sand,”*Geotextiles and Geomembranes*, vol. 19, no. 4, pp. 235–256, 2001.

[20] S. K. Dash, S. Sireesh, and T. G. Sitharam, (2003).”Behaviour of geocell-reinforced sand beds under circular footing,”*Ground Improvement*, vol. 7, no. 3, pp. 111–115, 2003.

[21] Raja, M.N.A., Shukla, S.K., 2020b. Ultimate bearing capacity of strip footing resting
on soil bed strengthened by wraparound geosynthetic reinforcement technique. Geotext. Geomembranes 48 (6), 867e874, https://doi.org/10.1016/j.geotexmem.2020.06.005.

[22] Raja MNA, Shukla SK, Experimental study on repeatedly loaded foundation soil strengthened by wraparound geosynthetic reinforcement technique, Journal of Rock Mechanics and Geotechnical Engineering, https://doi.org/10.1016/j.jrmge.2021.02.001

[23] Fragaszy RJ, Lawton E (1984).Bearing capacity of reinforced sand subgrades. J GeotechEng 110(10):1500–1507.

[24] Yetimoglu T, Wu JT, Saglamer A (1994).Bearing capacity of rectangular footings on geogrid–reinforced sand. J GeotechEng120(12):2083–2099.

[25] Akinmusuru JO, Akinbolade JA (1981).Stability of loadedfootings on reinforced soil. J GeotechGeoenvironmental Eng107(ASCE 16320 Proceeding).

[26] R.H. Myers, D.C. Montgomery, C.M. Anderson-Cook, (2016). Response surface methodology: process and product optimization using designed experiments, Wiley, New York. (2016).

[27] Sasmal, S. K., and R. N. Behera.(2018). “Prediction of Combined Static and Cyclic Load Induced Settlement of Shallow Strip Footing on Granular Soil Using Artificial Neural Network.” International Journal of Geotechnical Engineering 1–11. doi:10.1080/19386362.2018.1557384.

[28] Hamrouni A., Sbartai B., Dias D. (2021).”Ultimate dynamic bearing capacity of shallow strip foundations - Reliability analysis using the response surface methodology”.Soil Dynamics and Earthquake Engineering 144; 106690.

[29] Hamrouni A, Dias D, Sbartai B. (2020). Soil spatial variability impact on the behaviour of a reinforced earth wall. Front StructCivEng 2020:v15.

[30] Marandi, S.M., Anvar, M., and Bahrami, M., (2016). Uncertainty analysis of safety factor of embankment built on stone column improved soft soil using fuzzy logic α-cut technique. Computers and Geotechnics, 75, 135–144. doi:10.1016/j.compgeo.2016.01.014.

[31] Lafifi B, Rouaiguia A, Boumazza N (2019).Optimization of geotechnicalparameters using Taguchi’s design of experiment (DOE), RSM anddesirability function.InnovInfrastructSolut 4(1):1–12.

[32] ChanaPhutthananon, PornkasemJongpradist&Pitthay aJamsawang (2019): Influence of cap size and strength on settlements of TDM-piled embankments over soft ground,Marine Georesources & Geotechnology, DOI: 10.1080/1064119X.2019.1613700.

[33] Zhan J, Deng A, Jaksa M (2021).Optimizing micaceous soil stabilization using response surface method. J Rock MechGeotechEng 13(1): 212–220.

[34] Benayoun, F., Boumezerane, D., Bekkouche, S.R. *et al.*(2021). Optimization of geometric parameters of soil nailing using response surface methodology.*Arab J Geosci***14,** 1965 (2021). https://doi.org/10.1007/s12517-021-08280-z.

[35] Y.L. Kuo , M.B. Jaksa , A.V. Lyamin, W.S. Kaggwa(2009). ANN-based model for predicting the bearing capacity of strip footingon multi-layered cohesive soil, Computers and Geotechnics 36 (2009) 503–516.

[36] JahedArmaghani, D., Shoib, R.S.N.S.B.R., Faizi, K. *et al.* (2017).Developing a hybrid PSO–ANN model for estimating the ultimate bearing capacity of rock-socketed piles.Neural Comput&Applic**28,** 391–405 (2017). https://doi.org/10.1007/s00521-015-2072-z.

[37] Behera, R. N., C. R. Patra, N. Sivakugan, and B. M. Das. (2013). “Prediction of Ultimate Bearing Capacity of Eccentrically Inclined Loaded Strip Footing by ANN, Part I.” International Journal of Geotechnical Engineering 7 (1): 36–44. doi:10.1179/1938636212Z.00000000012.

[38] Sahu, R., C. R. Patra, N. Sivakugan, and B. M. Das.(2017b). “Bearing Capacity Prediction of Inclined Loaded Strip Footing on Reinforced Sand by ANN.” In International Congress and Exhibition” Sustainable Civil Infrastructures: Innovative Infrastructure Geotechnology”, 97–109. Cham: Springer.

[39] Acharyya R, DeyA (2018). Assessment of bearing capacity for strip footing located near sloping surface considering ANN model. Neural Comput Appl. https://doi.org/10.1007/s00521-018-3661-4.

[40] Acharyya R, Dey A, Kumar B (2018). Finite element and ANN-based prediction of bearing capacity of square footing resting on the crest of c-φ soil slope, International Journal of Geotechnical Engineering, DOI: 10.1080/19386362.2018.1435022.

[41] Sethy B.P, Patra C, Das B.C ,Sobhan K (2019). Prediction of ultimate bearing capacity of circular foundation on sand layer of limited thickness using artificial neural network, International Journal of Geotechnical Engineering, DOI: 10.1080/19386362.2019.1645437.

[42] Momeni, E., Armaghani, D.J., Fatemi, S.A. *et al.*(2018). Prediction of bearing capacity of thin-walled foundation: a simulation approach. *Engineering with Computers***34,** 319–327 (2018). https://doi.org/10.1007/s00366-017-0542-x.

[43] Acharyya, R., Dey, A. (2018).Assessment of bearing capacity of interfering strip footings located near sloping surface considering artificial neural network technique.*J.Mt. Sci.***15,** 2766–2780 (2018).https://doi.org/10.1007/s11629-018-4986-2.

[44] HosseinMoayedi, SajadHayati, (2018). Modelling and optimization of ultimate bearing capacity of strip footing near a slope by soft computing methods,Applied Soft Computing, Volume 66,2018,Pages 208-219,ISSN 1568-4946,https://doi.org/10.1016/j.asoc.2018.02.027.

[45] Muhammad Nouman Amjad Raja, Sanjay Kumar Shukla, *Geotextiles and Geomembranes*, https://doi.org/10.1016/j.geotexmem.2021.04.007

[46] Raja MNA, Shukla SK (2020). An extreme learning machine model for geosynthetic-reinforced sandy soil foundations. Proc Inst Civil Eng-Geotech Eng 175(4):383–403.

[47] Amjad Raja MN et al., Predicting and validating the load-settlement behavior of large-scale geosynthetic-reinforced soil abutments using hybrid intelligent modeling, Journal of Rock Mechanics and Geotechnical Engineering, https://doi.org/10.1016/j.jrmge.2022.04.012

[48] Khan, M.U.A., Shukla, S.K. & Raja, M.N.A (2022). Load-settlement response of a footing over buried conduit in a sloping terrain: a numerical experiment-based artificial intelligent approach. *Soft Comput* **26**, 6839–6856. https://doi.org/10.1007/s00500-021-06628-x

[49] Bardhan, A., Kardani, N., Alzo'ubi, A.K. et al(2022). A Comparative Analysis of Hybrid Computational Models Constructed with Swarm Intelligence Algorithms for Estimating Soil Compression Index. *Arch Computat Methods Eng***29**, 4735–4773. https://doi.org/10.1007/s11831-022-09748-1

[50] Bardhan, A.; Kardani, N.; Alzo'ubi, A.K.; Roy, B.; Samui, P.; Gandomi, A.H (2022). Novel Integration of Extreme Learning Machine and Improved Harris Hawks Optimization with Particle Swarm Optimization-Based Mutation for Predicting Soil Consolidation Parameter. *J. Rock Mech. Geotech. Eng.*, *14*, 1588–1608.

[51] Muhammad Nouman Amjad Raja, Sanjay Kumar Shukla & Muhammad Umer Arif Khan (2021): An intelligent approach for predicting the strength of geosynthetic-reinforced subgrade soil, International Journal of Pavement Engineering, DOI: 10.1080/10298436.2021.1904237.

[52] Bardhan A, GuhaRay A, Gupta S, Pradhan B, Gokceoglu C (2022). A novel integrated approach of ELM and modified equilibrium optimizer for predicting soil compression index of subgrade layer of dedicated freight corridor. Transp Geotech 32:100678.

[53] Hasthi V, Raja MNA, Hegde A, Shukla SK (2022). Experimental and intelligent modelling for predicting the amplitude of footing resting on geocell-reinforced soil bed under vibratory load. Transp Geotech 100783.

[54] Montgomery D (2001). Design and analysis of experiments. New York: John Wiley and Sons.

[55] S.A. Maruyama, S.V. Palombini, T. Claus, F. Carbonera, P.F. Montanher, N.E.D. Souza, M. Matsushita, Application of box-behnken design to the study of fatty acids and antioxidant activity from enriched white bread, J. Braz. Chem. Soc. 24 (9) (2013) 1520–1529.

[56] Zerti, A., Yallese, M.A., Meddour, I. *et al.*(2019). Modeling and multi-objective optimization for minimizing surface roughness, cutting force, and power, and maximizing productivity for tempered stainless steel AISI 420 in turning operations. *Int J AdvManuf Technol***102,** 135–157 (2019). https://doi.org/10.1007/s00170-018-2984-8

[57] Y. Nagata, K.H. Chu, (2003). Optimization of a fermentation mediumusing neural networks and genetic algorithms. Biotechnol.Lett.25, 1837–1842 (2003).

[58] B. Sarkar, A. Sengupta, S. De et al.,(2009). Prediction of permeatefluxduring electric field enhanced cross-flow ultrafiltration a neuralnetwork approach. Sep. Purif. Technol. 65, 260–268 (2009).

[59] Meddour, I., Yallese, M.A., Bensouilah, H. *et al.*(2018). Prediction of surface roughness and cutting forces using RSM, ANN, and NSGA-II in finish turning of AISI 4140 hardened steel with mixed ceramic tool.*Int J AdvManuf Technol***97,** 1931–1949 (2018). https://doi.org/10.1007/s00170-018-2026-6.

[60] Kalman BL, Kwasny SC (1992). Why Tanh: choosing a sigmoidalfunction, Proc. Int. Jt. Conf Neural Network. Baltimore, 4 578–581.

[61] Labidi, A., Tebassi, H., Belhadi, S. *et al.*(2018). Cutting Conditions Modeling and Optimization in Hard Turning Using RSM, ANN and Desirability Function. *J Fail. Anal.and Preven.***18,** 1017–1033 (2018).https://doi.org/10.1007/s11668-018-0501-x

[62] M. Ramezani, A. Afsari, (2015). Surface roughness and cutting forceestimation in the CNC turning using artificial neural networks.Manag. Sci. Lett. 5, 357–362 (2015).

[63] M. Rajendra, P.C. Jena, H. Raheman, (2009). Prediction of optimizedpretreatment process parameters for biodiesel production usingANN and GA. Fuel 88, 868–875 (2009).

[64] R.M. Garcia-Gimeno, C. Hervas-Martinez, R. Rodriguez-Perezetal.,(2005). Modelling the growth of Leuconostocmesenteroidesbyartificial neural networks.Int. J. Food Microbiol.105, 317–332(2005).

[65] K.R. Kashyzadeh, E. Maleki, (2017).Experimental investigation andartificial neural network modeling of warm galvanization andhardened chromium coatings thickness effects on fatigue life ofAISI 1045 carbon steel. J. Fail. Anal.Prev. 17(6), 1276–1287(2017).

[66] Huang, C., and Tatsuoka, F. 1990. "Bearing capacity of reinforced horizontal sandy ground."*Geotext.Geomembr.*, 9, 51–80.

[67] Khing, K. H., Das, B. M., Puri, V. K., Cook, E. E., and Yen, S. C. 1993."The bearing capacity of a strip foundation on geogridreinforcedsand."*Geotext.Geomembr.*, 124, 351–361.
[68] Shin, E. C., Das, B. M., Lee, E. S., and Atalar, C. 2002. "Bearingcapacity of strip foundation on geogrid-reinforced sand."*Geotech.Geologic. Eng.*, 20, 169–180.
[69]Cicek E, Guler E, Yetimoglu T (2015).Effect of reinforcementlength for different geosynthetic reinforcements on strip footing on sand soil. Soils Found 55(4):661–677.
[70] El Sawwaf M, Nazir AK (2010). Behavior of repeatedly loadedrectangular footings resting on reinforced sand. Alex EngJ49(4):349–356. https://doi.org/10.1016/j.Egg.2010.07.002
[71] Abu El-Soud S, BelalAM (2019).Numerical modeling of rigid stripshallow foundations overlaying geosythetics-reinforced loosefine sand deposits.Arab J Geosci.https://doi.org/10.1007/s12517-019-4436-7
[72] Akinmusuru, J. O., and Akinboladeh, J. A. (1981). "Stability of loadedfootings on reinforced soil."*J. Geotech. Engrg.Div.*, 1076, 819–827.
[73] Das, B. M., and Omar, M. T. (1994). "The effects of foundation width onmodel tests for the bearing capacity of sand with geogrid reinforcement."*Geotech.Geologic. Eng.*, 12, 133–141.
[74] El Sawwaf, M. 2007. "Behavior of strip footing on geogrid-reinforcedsand over a soft clay slope."*Geotext.Geomembr.*, 25, 50–60.
[75] Boushehrian J, Hataf N. (2003).Experimental and numerical investigation of the bearing capacity of model circular and ring footing on reinforced sand. Geotextiles andGeomembranes 2003;21(4):241e56.
[76] Mosallanezhad M, Hataf N, Ghahramani A. (2008). Experimental study of bearing capacityof granular soils reinforced with innovative grid-anchor system. Geotechnicaland Geological Engineering 2008;26(3):299e312.
[77] Latha M, Somwanshi A. (2009).Effect of reinforcement form on the bearing capacity of square footings on sand. Geotextiles and Geomembranes 2009;27(6):409e22.
[78] DeMerchant MR, Valsangkar AJ, Schriver AB (2002). Plate loadtests on geogrid reinforced expanded shale lightweight aggregate. GeotextGeomembr 20:173–190.
[79] A.I Khuri, S. Mukhopadhyay, (2010).Response surface methodology, WIREs. Comput. Stat. 2 (2010)128-149.
[80] R.H. Myers, D.C. Montgomery, (2002). Response surface methodology: process and product optimization using designed experiments, 2nd ed. John Wiley and Sons, Inc. New York. (2002).
[81] A.K. Sahoo, P.C. Mishra, (2014). A response surface methodology and desirability approach for predictive modeling and optimization of cutting temperature in machining hardened steel, Inter. J. Indus. Eng. Comp. 5 (2014) 407-416.
[82] Bardhan, A.; Kardani, N.; Alzo'ubi, A.K.; Roy, B.; Samui, P.; Gandomi, A.H. Novel Integration of Extreme Learning Machine and Improved Harris Hawks Optimization with Particle Swarm Optimization-Based Mutation for Predicting Soil Consolidation Parameter. *J. Rock Mech. Geotech. Eng.* **2022**, *14*, 1588–1608.
[83] Khellaf A., Aouici H., Smaiah S., Boutabba S., Yallese M. A., Elbah M., (2016). Comparative assessment of two ceramic cutting tools on surface roughness in hard turning of AISI H11 steel: including 2D and 3D surface topography, Int J AdvManufTechnol, 10.1007/s00170-016-9077-3.
[84] Reddy NSK, Rao PV (2005). Selection of optimum tool geometry and cutting conditions using a surface roughness prediction model for end milling.Int J AdvManufTechnol 26(11–12):1202–1210.